CHAPTER III

RESULTS AND DISCUSSION

3.1 CE Conditions and Optimisation

3.1.1 CE conditions

In this work, CE conditions for analysis of GA_3 were selected using a 57 cm in length (50 cm to detector) × 50 μm I.D. uncoated fused silica capillary and background electrolyte (BGE) as a borate buffer at pH 9.2. GA_3 is an acidic compound with pK_a 3.8 [Tian *et al.* 2003]. Therefore, the BGE at basic pH was chosen to allow GA_3 having a negative charge and to generate high EOF enough for carrying negatively charged GA_3 toward the detector because the electrophoretic mobility of GA_3 has the opposite direction with EOF, as seen in Figure 1.5 and Equation 1.10. Both electrophoretic mobility and EOF affect the migration time of analyte and depend on the pH of BGE, and therefore the buffer is necessary for CE analysis to maintain the constant pH. $Na_2B_4O_7$ dissolved in water is widely used as the basic BGE since it provides a buffer at pH 9.2 without adjusting pH [Altria and Fabre 1995]. It can be explained by the equation

$$Na_2B_4O_7 + 7H_2O \longrightarrow 2Na^+ + 2H_3BO_3 + 2B(OH)_4^- \qquad (3.1)$$

The pH of a solution containing weak acid (HA) and conjugated base (A^-) is given by the Henderson-Hasselbalch equation [Chang 1991]

$$pH = pK_a + \log\frac{[A^-]}{[HA]} \qquad (3.2)$$

In this case, HA is H_3BO_3 and A^- is $B(OH)_4^-$. As seen in Equations 3.1 and 3.2, the same concentrations of H_3BO_3 and $B(OH)_4^-$ provide high buffering capacity. As a result, the same concentration of the borate buffer prepared from $Na_2B_4O_7$ leads to precision in electrophoretic mobility, EOF and migration time. In addition, $Na_2B_4O_7$

is available in highly pure reagent grade, and the borate buffer is easy to prepare and stable for a long period of time [Chankvetadze 1997]. An uncoated fused silica capillary, similar to that used in GC, is the most popular for CE. It is a good material due to its UV transparency and durability when polyimide coated [Weinberger 1993]. Although fused silica capillaries for CE are commercially available with internal diameters ranging from 20 to 200 μm, the most commonly used capillary dimensions are 25, 50 and 75 μm I.D. [Chankvetadze 1997]. The 25 μm I.D. capillary provides high resolution and less Joule heating, but results in analyte-capillary wall interaction, especially cationic analyte, due to its small internal diameter. In addition, the use of very small diameter capillary always has problems with low detection sensitivity due to small path length of light rays and with clogging of the capillary. The 75 μm I.D. capillary provides low wall interaction and high sensitivity but may cause low resolution due to peak broadening caused by Joule heating ($\sigma^2_{th} \propto r^6$ as seen in Equation 1.24). In addition, it has limitation of the use of high BGE concentration which can reduce electromigration dispersion and the use of high voltage which can reduce peak broadening due to diffusion. Therefore, 75 μm I.D. capillary is usually used to improve detection sensitivity and decrease wall interaction when separations have no problem of resolution. Typically, the 50 μm I.D. capillary is used for many applications due to its compromise among resolution, sensitivity, heat dissipation and wall interaction. This work does not involve analysis of trace levels of GA_3, therefore, the 50 μm I.D. capillary was selected. For length of the capillary, the total length of capillary (L) is important for the field strength. In CE, the length of capillary is usually used in the range of 30 to 60 cm. The longer the capillary length, the greater the migration time of analyte. The shorter capillary gives faster analysis time but poorer resolution. To obtain suitable analysis time and efficiency, a capillary with 57 cm in length (50 cm to detector) was used.

3.1.2 CZE optimisation

In initial work, CZE with the BGE as a borate buffer at pH 9.2 was used for determination of GA_3 in fermentation broth. In production of GA_3 at IBGE, typically, GA_3 is isolated from the 10-day fermentation broth, and therefore, the 10-day fermentation broth was 10 times diluted with water, and used for investigation on suitable CZE conditions for separation of GA_3 from other compounds in the broth. Effects of BGE concentration and applied voltage on the separation of GA_3 were studied by varing the buffer concentration in the range of 12.5 to 50 mM using the separation voltages at 25 and 30 kV. Figures 3.1 and 3.2 show an example of electropherograms of the 10-day fermentation broth diluted 10 times using the separation voltages of 25 and 30 kV, respectively. By spiking standard GA_3 into the diluted fermentation broth, the peak 1 was identified to be GA_3. As seen in Figure 3.1, there is a small unknown peak 2 close to the GA_3 peak.

The first consideration is given to the migration behaviour of GA_3 caused by varying the BGE concentration and separation voltage. Figures 3.3 to 3.5 show electroosmotic mobility (μ_{eo}), electrophoretic mobility (μ) and total mobility (μ_{net}) of GA_3, respectively. Electroosmotic mobility is calculated using Equation 1.10, where t_{eo} is the migration time of the EOF marker obtained from the first migrating order of electropherograms in Figure 3.1. At a fixed BGE concentration, when the separation voltage was increased from 25 to 30 kV, an increase of μ_{eo} was obtained due to Joule heating leading to a decrease in the BGE viscosity ($\mu_{eo} \propto 1/\eta$ as shown in Equation 1.7). In consistent with theory, μ_{eo} in Figure 3.2 was found to decrease with an increase in the ionic strength of BGE due to a decrease in zeta potential ($\mu_{eo} \propto \zeta$ as shown in Equation 1.7). Theoretically, the greater the BGE concentration or conductivity, the greater the heat generating. However, results in this experiment showed that a decrease in μ_{eo} was influenced by a decrease in zeta potential more than an increase in Joule heating. To confirm Joule heating in this work, experimental and predicted values of electric current (I_A) are compared in Figure 3.6. The predicted current is calculated using Equation 3.3 [Feret 1993]

$$I_A = \kappa_s ES \tag{3.3}$$

where κ_s is the BGE conductivity, E the electric field strength, and S the cross-section area of the capillary. κ_s is given by Equation 3.4

$$\kappa_s = F\Sigma z_i c_i \mu_i \tag{3.4}$$

In this case, $\Sigma z_i c_i \mu_i$ is equal to $c_{Na+}\mu_{Na+} + c_{B(OH)4-}\mu_{B(OH)4-}$. The μ_i at a given ionic strength of the BGE is calculated using the equation linking the observed electrophoretic mobility (μ) with the absolute mobility (mobility at zero ionic strength, μ^o) [Survay *et al.* 1996]

$$\mu = \mu^o - \left(3.13 + 0.23\mu^o\right)\frac{\sqrt{I}}{1+3.29a\sqrt{I}} \tag{3.5}$$

μ^o values of Na^+ and $B(OH)_4^-$ are 5.3×10^{-8} and -4.00×10^{-8} $m^2\ V^{-1}\ s^{-1}$, respectively [Pospíchal *et al.* 1989]. In this Equation, a (nm) is the sum of the hydrodynamic radii (r_h) of analyte ion and counter ion. In this case, a is the sum of r_h of Na^+ and $B(OH)_4^-$. r_h may be calculated from the absoluted mobility [Survay *et al.* 1996].

$$r_h = \frac{ze}{6\pi\eta\mu^o} \tag{3.6}$$

The parameters in Equation 3.6 are previously defined as shown in Equation 1.4. In using Equations 3.4-3.6, electrophoretic mobility and charge are used as unsigned quantities through out, i.e. the modulus of μ and z.

From Figure 3.6, at a fixed voltage, the experimental (▲ and ■) higher than predicted (△ and □) current is found. When the ionic strength of the BGE increases from 25 to 100 mM, the ratio of experimental and predicted current is found to increase from 1.11 to 1.22 for separation voltage of 25 kV and from 1.12 to 1.29 for 30 kV. This indicates that Joule heating increases with an increase in the ionic strength of BGE and separation voltage.

The total electrophoretic mobility (μ_{net}) and electrophoretic mobility of GA_3 shown in Figures 3.4 and 3.5 were calculated using Equations 1.11 and 1.9, respectively, where t_m is obtained from electropherograms in Figures 3.1 and 3.2. As previously mentioned in Section 3.1.1, GA_3 carries a negative charge and migrates opposite direction of EOF. Therefore, under high EOF and normal polarity (detection), GA_3 passes through a detector after the EOF marker. It is seen in Figure 3.5 that, at separation voltage of 25 kV, electrophoretic mobility slightly decreases with an increase in the BGE ionic strength due to a decrease in an effective charge of GA_3 and an increase of the size of ionic GA_3 surrounded with counter ion Na^+. However, at the separation voltage of 30 kV, insignificant difference in electrophoretic mobility of GA_3 is found with an increase of the BGE ionic strength, in the range of 25 to 100 mM, due to the opposite dual effects of Joule heating, leading to an increase of μ, and an increase of ionic strength, leading to a decrease of μ. To confirm the effect due only to Joule heating, the electrophoretic mobilities (μ) of GA_3 at a given ionic strength (black symbols) were corrected to those (μ^o) at zero ionic strength (blank symbols) using Equations 3.5 and 3.6, where a is now the sum of r_h between GA_3 and Na^+. Theoretically, the BGE ionic strength does not affect a change of μ^o because μ^o is calculated at the zero ionic strength of the BGE. However, results in Figure 3.4 show that μ^o (blank symbols) increases with an increase of the BGE ionic strength. It can be explained that this phenomena is affected by the Joule heating caused by an increase of the BGE conductivity or ionic strength. In addition, the higher the separation voltage, the grater the Joule heating.

As seen in Figure 3.5, the total mobility of GA_3 is found to decrease with an increase of the BGE ionic strength due to a significant decrease of EOF (Figure 3.3) and insignificant change of electrophoretic mobility of GA_3 (black symbols in Figure 3.4). The decrease in the total mobility leads to a long migration time of GA_3 as shown in Figures 3.1 and 3.2. In comparison with the separation voltage of 30 kV, that of 25 kV gives longer migration time due to $t_m \propto 1/V$.

The next consideration is given to the peak variance and peak shape of GA_3 as shown in Tables 3.1 and 3.2. The predicted peak variances due to diffusion (σ^2_{diff}) and electromigration dispersion (σ^2_{EMD}) are calculated using Equations 1.21 and 1.26,

respectively. The predicted value of σ^2_{tc} in Table 3.1 is the peak variance due to the time constant effect caused by an *RC* circuit which is an electronic filter applied to the detector output to reduce noise. The product *RC* is called time constant (τ_{tc}), where *R* is the resistance and *C* the capacitance [Horowitz and Hill 1989]. The greater the time constant, the lower the noise. However, the time constant effect gives a broader and tailing peak, and its contribution to variance is given by Equation 3.7 [Reijenga and Kenndler 1994]

$$\sigma^2_{tc} = \left(\frac{\tau_{tc} l}{t_m} \right)^2 \tag{3.7}$$

The observed peak variance is obtained from the measurement of the peak width at base ($\sigma = w_b/4$) in electropherograms in Figures 3.1 and 3.2. σ in the distance unit is equal to σ in the time unit multiplied by the v_{net} of GA_3. The asymmetry factor (A_{asym}) in Table 3.2 is equal to *b/a*, where *a* is the distance between the peak front and the peak maximum, and *b* the distance between the peak maximum and the peak end, measured at 10 % of the peak height [Robards *et al.* 1994]. For electropherogram in the time domain, $A_{asym} < 1$ indicates the fronting peak, while $A_{asym} > 1$ indicates the tailing peak. The percentage of EMD (P_{EMD}) in Table 3.2 is defined as $100\sigma^2_{EMD}/\sigma^2_{tot}$, where σ^2_{tot} in this work is the observed value obtained from the electropherograms in Figures 3.1 and 3.2. The value of P_{EMD} or triangular distribution can be used to indicate the distortion of peak. The smaller the value of P_{EMD}, the smaller the distortion of peak. For P_{EMD} = 10% or the percentage of Guassian variance = 90%, the peak almost has Guassian shape [Erny *et al.* 2001].

From Table 3.1, the predicted σ^2_{diff} is seen to increase with an increase in the BGE ionic strength and a decrease of applied voltage, due to an increase of the migration time of GA_3. As previously discussed in Section 1.2.5.3, EMD causes triangular distribution of CE peak. At 12.5 mM $Na_2B_4O_7$ or the ionic strength of 25.0 mM, the electrophoretic mobility of GA_3 shown in Figure 3.1a was observed to be -1.62×10^{-8} $m^2\ V^{-1}\ s^{-1}$ and the electrophoretic mobility of a borate ion, $B(OH)_4^-$, as the BGE co-ion is calculated to be -3.36×10^{-8} $m^2\ V^{-1}\ s^{-1}$ using absolute electrophoretic mobility of -4.00×10^{-8} $m^2\ V^{-1}\ s^{-1}$ [Survay *et al.* 1996] and Equation 3.5. Mismatch between

electrophoretic mobilities of the analyte and the BGE co-ion causes EMD, leading to distortion of GA_3 peak [Khaledi 1998]. From the GA_3 peak shape in Figures 3.1 and 3.2 and $A_{asym} < 1$ (except for the BGE ionic strength of 100 mM) in Table 3.2, the GA_3 peak has fronting distribution. This may be explained that, in this case, μ of GA_3 is less than μ of $B(OH)_4^-$ as the BGE co-ion, and the direction of μ for GA_3 and the BGE co-ion is backward the inlet capillary end. The BGE co-ion can enter the front of the analyte zone, resulting in the fronting distribution of the analyte peak [Chankvetadze 1997]. At the BGE ionic strength of 100 mM, the value of A_{asym} slightly higher than 1 is possibly due to the experimental error of $A_{asym} \sim 1.0$ or the effect of the time constant which gives tailing peak or $A_{asym} > 1$ in the time domain [Jeansonne and Foley 1991]. The predicted σ^2_{EMD} in Table 3.1 and the percentage of EMD (P_{EMD}) in Table 3.2 were found to decrease with an increase of the BGE ionic strength. This can be explained by the fact that an increase of the BGE concentration results in a decrease of the conductivity difference between the BGE zone and the analyte zone or a decrease of the parameter of a_A in Equation 1.27, leading to a decrease of σ^2_{EMD}. At the BGE ionic strengths of 80 mM and 100 mM, the P_{EMD} nearly 10% was found to be in agreement with $A_{asym} \sim 1.0$, indicating that the GA_3 almost has Gaussian shape.

In this experiment, the rise time of 1 s or time constant of 1/2.2 was used to reduce noise. As shown in Table 3.1, the predicted σ^2_{tc} calculated using Equation 3.7 is found to decrease with an increase of the BGE ionic strength and a decrease of applied voltage due to an increase of the migration time of GA_3. Other sources of peak variance are negligible, such as detector aperture width, thermal dispersion and injection length after sample stacking, with each predicted $\sigma^2 < 0.05 \times 10^{-6}$ m^2.

As shown in Table 3.2, at each CE condition, the observed peak variance is seen to be approximately twice the predicted values. This may be the additional contributions to peak variance due to a parabolic profile of the analyte zone caused by the mismatch of EOF in the sample plug and the BGE zone [Burgi and Chien 1991] and the difference in the temperature between a thermostatted section and unthermostatted sections [Nhujak 2001a], which their peak variances cannot be predicted exactly. In the range of 25 to 80 mM ionic strength of the BGE, the observed peak variance was found to

decrease with an increase of the BGE concentration and to have a similar trend of the sum of predicted peak variance of σ^2_{diff}, σ^2_{EMD} and σ^2_{tc}. The greater observed peak variance at the BGE ionic strength of 100 mM than that at 80 mM may be due to the significant effect of Joule heating and the greater difference in the temperature in the capillary sections as previously mentioned.

The consideration is now given to peak efficiency (N) of GA_3 and resolution of GA_3 and unknown peak 2. The values of N in Table 3.3 were obtained from the observed peak variance and Equation 1.13. Since N is proportional to $1/\sigma^2$, the smaller the value of σ^2, the greater the value of N. The effect of the BGE ionic strength and the applied voltage on N can be explained in the similar way to the peak variance. The resolution in Table 3.3 was obtained from the electropherograms in Figures 3.1 and 3.2 and Equation 1.16. Baseline resolution of GA_3 and unknown peak 2 was found to increase with an increase of BGE concentration mainly due to a decrease in peak variance due to EMD as shown in Table 3.1, leading to improvement of resolution. A change of the BGE concentration from 40 to 50 mM results in a slight decrease of N but a slight increase of R_s. It should be noted from Equation 1.18 that R_s is also proportional to the reciprocal of the total mobility. Results from Figure 3.3 show that 50 mM $Na_2B_4O_7$ gives the smaller the total mobility, leading to an increase of R_s. From Table 3.3, at a fixed BGE concentration, insignificant difference of resolution of GA_3 and unknown peak 2 was obtained when using the separation voltages of 25 and 30 kV. This may be due to small effect of σ^2_{th}.

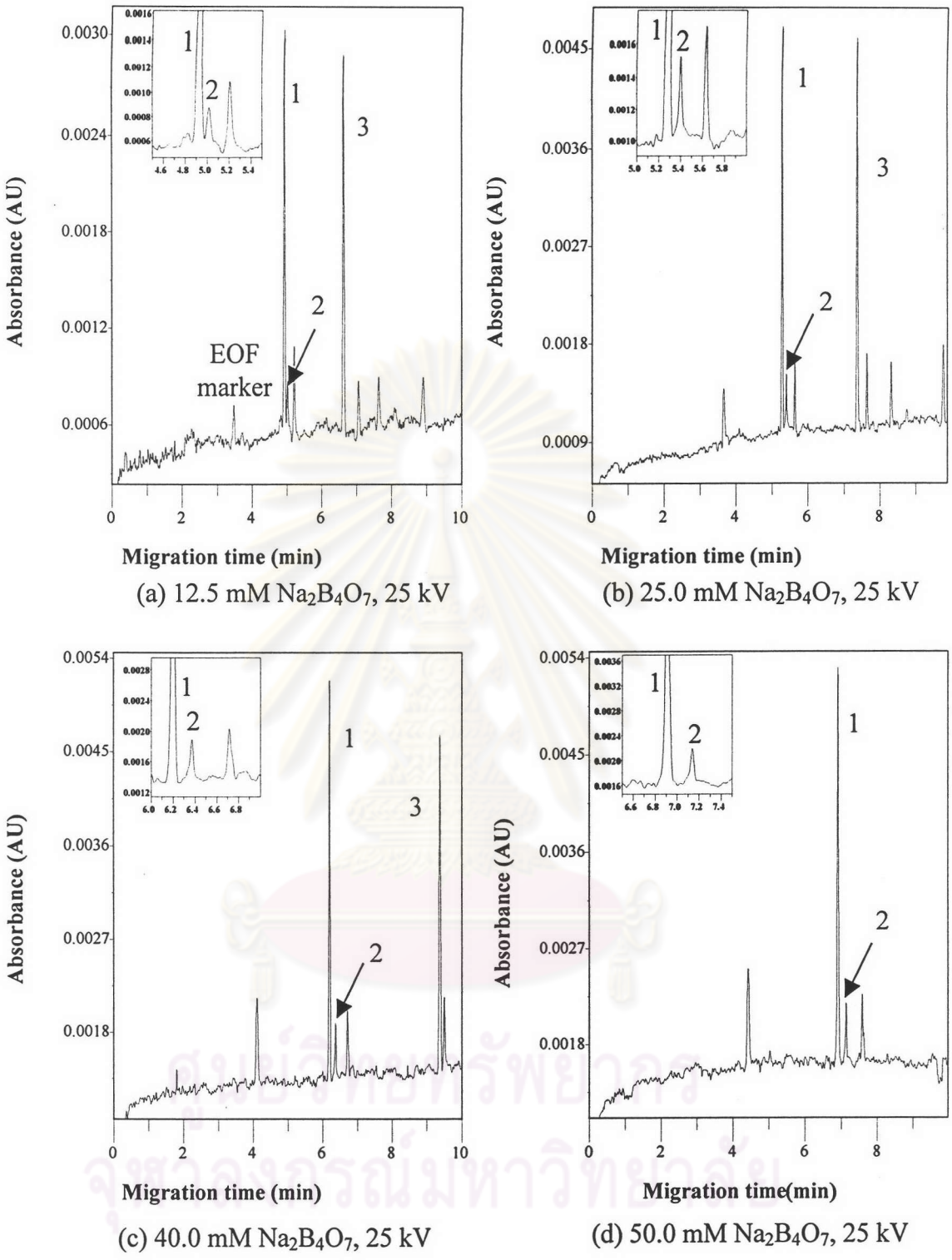

Figure 3.1 An example of electropherograms of the 10-day fermentation broth diluted 10 times using separation votage of +25 kV and BGE concentrations of (a) 12.5, (b) 25.0, (c) 40.0 and (d) 50.0 mM. Peak 1 = GA_3, 2 = unknown, 3 = AMBA and 4 = unknown. Other CE conditions: uncoated fused silica capillary 50 μm I.D. × 57 cm (50 cm to detector), temperature of 25 °C, 0.5 psi pressure injection for 4 s and UV detection at 214 nm.

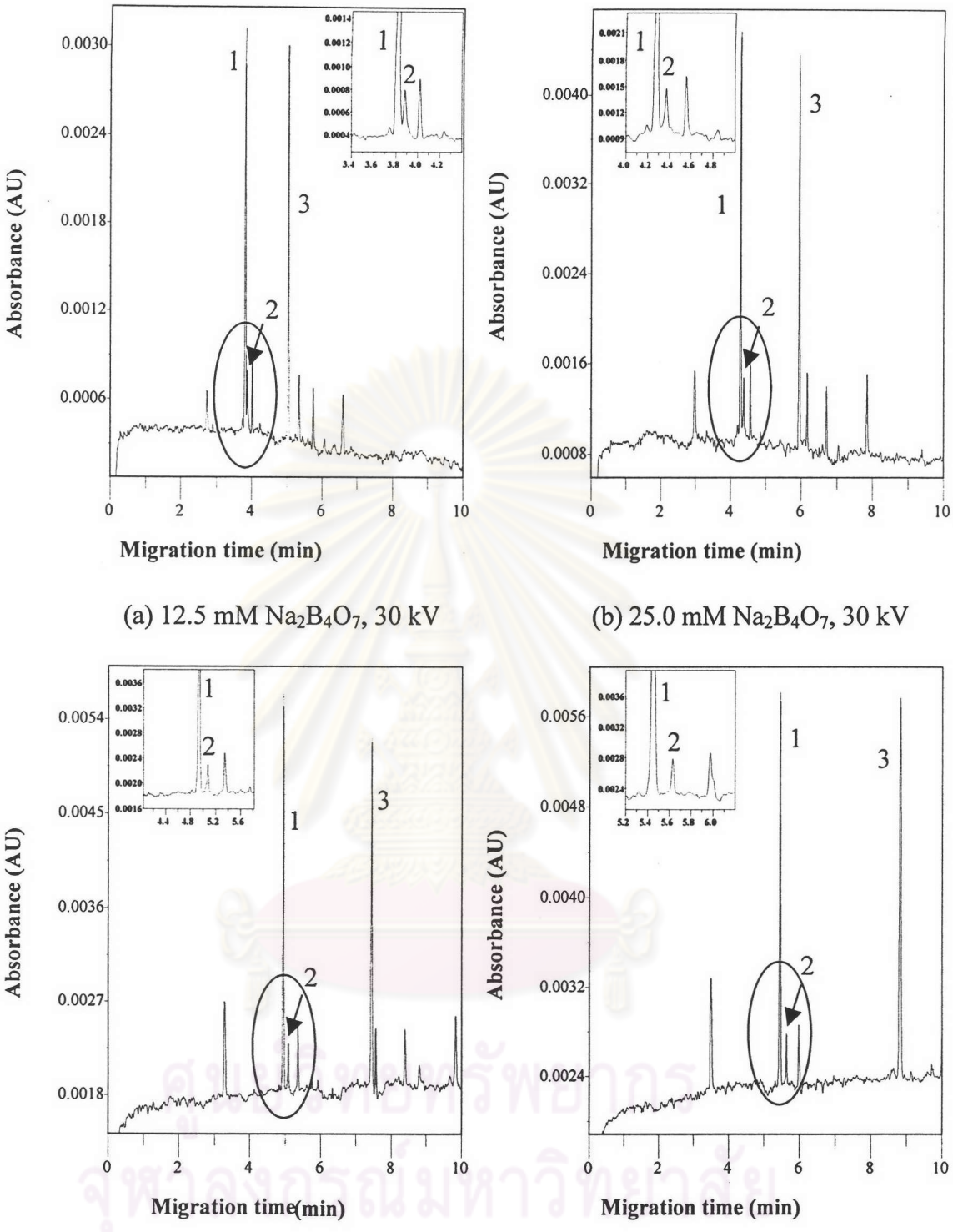

Figure 3.2 An example of electropherograms of the 10-day fermentation broth diluted 10 times using the separation voltage of +30 kV, BGE concentrations of (a) 12.5, (b) 25.0, (c) 40.0 and (d) 50.0 mM. Peak 1 = GA_3, 2 = unknown and 3 = AMBA. Other CE conditions as shown in Figure 3.1.

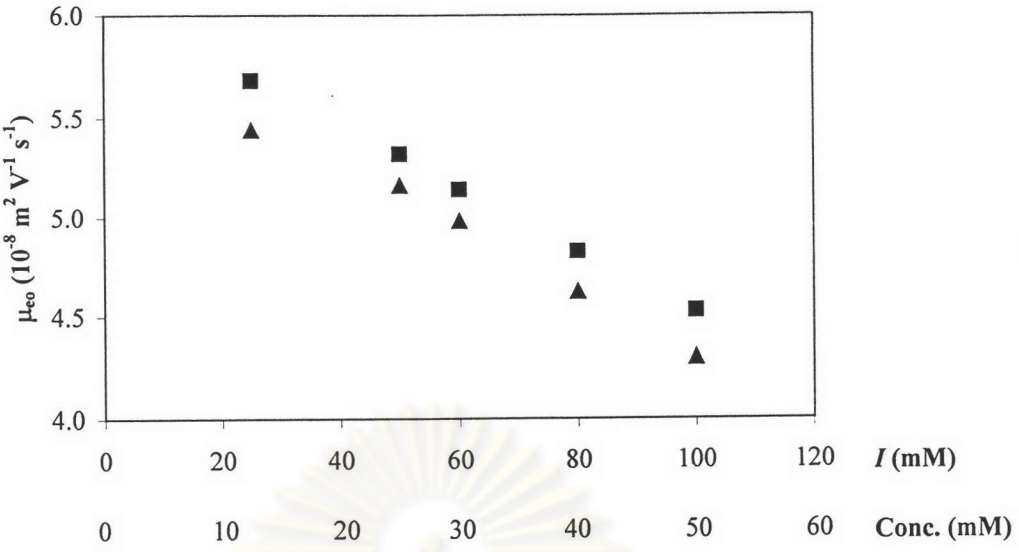

Figure 3.3 Effect of BGE ionic strength (*I*) on electroosmotic mobility (μ_{eo}) at separation voltage of +25 (▲) and +30 kV (■). Other CE conditions as shown in Figure 3.1.

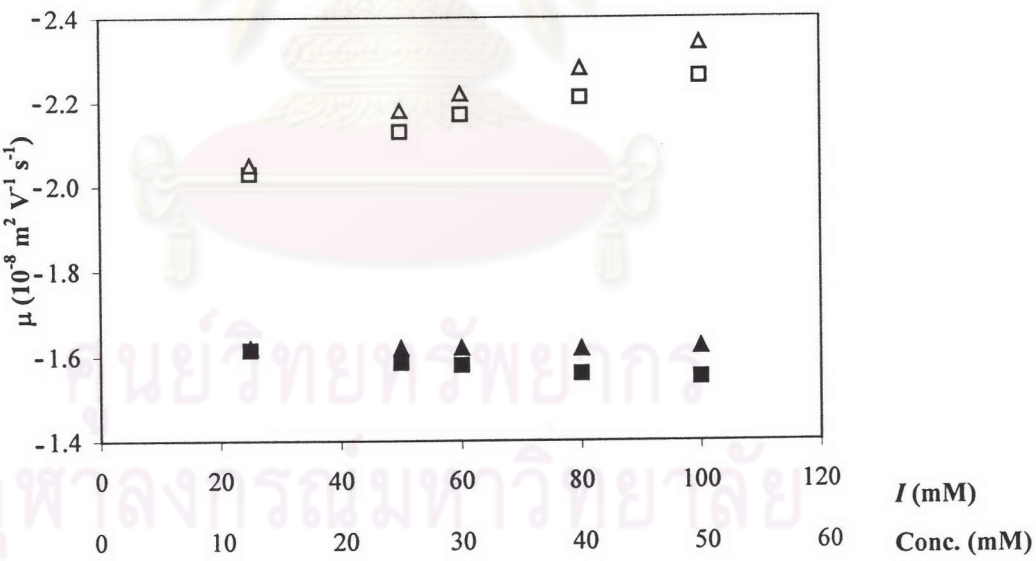

Figure 3.4 Effect of BGE ionic strength (*I*) on electrophoretic mobility (μ). Symbols: (■) μ at +25 kV; (▲) μ at +30 kV; (□) μ^o at +25 kV; (△) μ^o at +30 kV. Other CE conditions as shown in Figure 3.1.

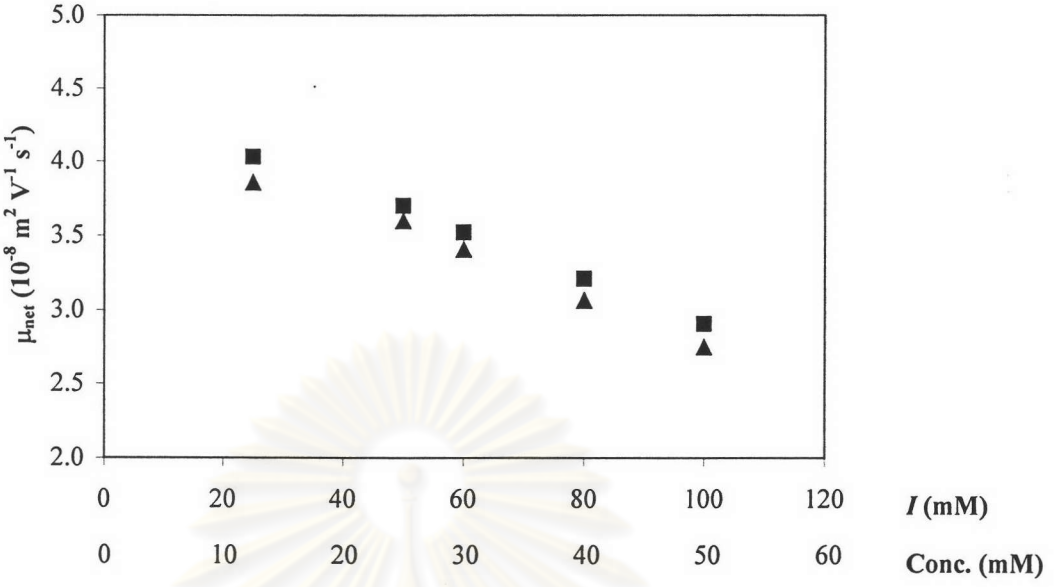

Figure 3.5 Effect of BGE ionic strength (I) on total mobility (μ_{net}) at separation voltage of +25 (▲) and +30 kV (■). Other CE conditions as shown in Figure 3.1.

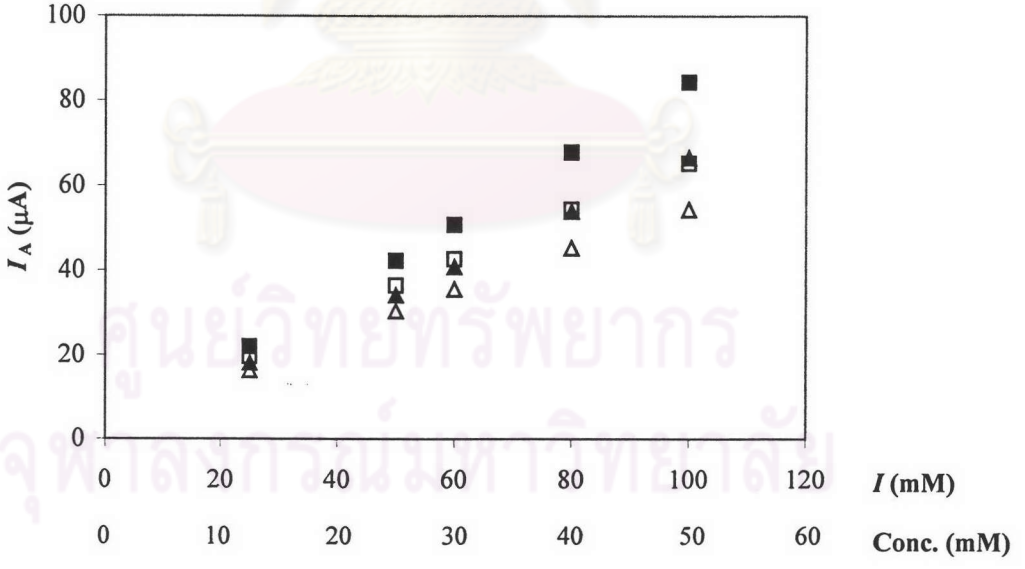

Figure 3.6 Effect of BGE ionic strength (I) on electric current (I_A) at separation voltage of +25 (▲) and +30 kV (■). Symbols △ and □ are the predicted values of I_A at separation voltage of +25 and +30 kV, respectively. Other CE conditions as shown in Figure 3.1.

Table 3.1 Observed and predicted peak variances (σ^2) of GA_3

BGE (mM)	25 kV				30 kV			
	Predicted σ^2 (10^{-6} m^2)			Observed σ^2_{tot} (10^{-6} m^2)	Predicted σ^2 (10^{-6} m^2)			Observed σ^2_{tot} (10^{-6} m^2)
	σ^2_{diff}	σ^2_{EMD}	σ^2_{tc}		σ^2_{diff}	σ^2_{EMD}	σ^2_{tc}	
12.5	0.31	1.03	0.58	3.78 ± 0.58	0.30	0.98	0.93	3.82 ± 0.66
25.0	0.35	0.51	0.51	2.18 ± 0.16	0.34	0.49	0.78	2.50 ± 0.16
30.0	0.37	0.44	0.46	2.12 ± 0.10	0.36	0.42	0.71	2.20 ± 0.25
40.0	0.42	0.36	0.37	1.98 ± 0.06	0.41	0.31	0.59	2.16 ± 0.14
50.0	0.48	0.31	0.30	2.35 ± 0.17	0.47	0.28	0.48	2.34 ± 0.22

Table 3.2 The percentage of σ^2_{EMD} (P_{EMD}) and peak asymmetry factor (A_{asym}) of GA_3

BGE (mM)	P_{EMD}		A_{asym}	
	25 kV	30 kV	25 kV	30 kV
12.5	27.3	25.5	0.72 ± 0.04	0.73 ± 0.03
25.0	23.4	19.6	0.74 ± 0.01	0.76 ± 0.01
30.0	20.8	19.0	0.76 ± 0.01	0.79 ± 0.02
40.0	17.9	15.3	0.88 ± 0.03	0.91 ± 0.09
50.0	13.1	12.0	1.11 ± 0.01	1.16 ± 0.08

Table 3.3 Peak efficiency (N) of GA_3 and resolution (R_s) of GA_3 and unknown peak 2

BGE (mM)	R_s		N (10^5)	
	25 kV	30 kV	25 kV	30 kV
12.5	1.11 ± 0.03	1.04 ± 0.02	0.67 ± 0.08	0.66 ± 0.07
25.0	1.56 ± 0.01	1.51 ± 0.01	1.15 ± 0.08	1.00 ± 0.06
30.0	1.69 ± 0.04	1.58 ± 0.09	1.18 ± 0.05	1.15 ± 0.13
40.0	1.90 ± 0.25	1.98 ± 0.20	1.26 ± 0.04	1.16 ± 0.07
50.0	2.04 ± 0.01	2.38 ± 0.01	1.06 ± 0.08	1.07 ± 0.10

3.1.3 MEKC optimisation

To compare with CZE, MEKC for separation of GA_3 and other compounds was carried out using SDS as micellar phase. The SDS is the most widely used anionic surfactant for MEKC due to its high water solubility and lipid-solubilising power [Weinberger 1993]. Because of its widespread applicability, this SDS surfactant is available in highly purified form and is inexpensive. Effect of SDS concentration on the separation of GA_3 and other compounds was investigated using the Na_2B4O_7 concentration of 25.0 mM and the applied voltage of 30 kV and varying SDS concentration in the range of 20 to 150 mM. Since the critical micellar concentration (CMC) of SDS is equal to 8.1 mM [Khaledi 1998], the SDS concentration greater than CMC is required to obtain stable micellar phase in MEKC. Typically, addition of SDS in the borate buffer results in an increase of the BGE ionic strength, therefore, the lower concentration of buffer in MEKC (25.0 mM Na_2B4O_7) than that in CZE (40.0 mM Na_2B4O_7) were selected to keep Joule heating minimum. MEKC electropherograms of the fermentation broth diluted 10 times are shown in Figure 3.7. It should be noted that CZE and MEKC experiments were performed using different batches of the fermentation broth.

Peak 3 in Figure 3.7 belongs to 3-amino-4-methylbenzoic acid (AMBA) spiked as an internal standard for quantitative analysis in the following section. From Figure 3.7, an increase in the SDS concentration resulted in the better resolution of GA_3 and unknown peak 2. However, at above 40 mM SDS concentration, another unknown peak 4 separating from the GA_3 peak was observed. The amount of analyte injected is proportional to corrected peak area, A_{corr}, peak area divided by migration time. The values of A_{corr} for peak GA_3 in Figures 3.7a and 3.7d were found to be 23.33 and 14.57 μAU. This indicates that peak GA_3 in Figure 3.7a belongs to GA_3 peak overlapping unknown peak 4. Above 100 up to 150 mM SDS, no unknown peak separating from peak GA_3 was observed. To explain the effect of SDS concentration on the resolution of GA_3 and other unknown compounds in the broth, MEKC behaviours of GA_3 and unknown compounds 2 and 4 are firstly discussed.

Figures 3.8 to 3.10 show the effect of SDS on the electroosmotic mobility, electrophoretic mobilities and total mobilities of interested compounds. From Figure 3.8, at the fixed concentration of $Na_2B_4O_7$, the electroosmotic mobility is seen to be insignificantly different with an increase in the SDS concentration above 20 mM. Terabe *et al.* [1985] demonstrated that changes in SDS concentration above the CMC (8.1 mM) resulted in no significant change in electroosmotic mobility due to insignificant difference of the zeta potential at the solution-capillary wall interface. This may be explained that, at above CMC, Na^+ ions from SDS act as counter ions for dodecylsulfate ions and do not form the double layer near the negatively charged capillary wall, resulting in no change in the zeta potential ($\mu_{eo} \propto \zeta$ as shown in Equation 1.7). This situation is contrast to an increase of $Na_2B_4O_7$ causing a decrease in μ_{eo} as seen in Figures 3.3 and 3.9.

As previously mentioned in Equation 1.38, at a given SDS concentration, the observed electrophoretic mobility of the analyte ($\mu_{obs,A}$) is equal to the sum of electrophoretic mobility of free analyte and analyte:SDS complex weighted according to the mole fraction. Typically, the electrophoretic mobility of analyte:SDS complex is assumed to be equal to the electrophoretic mobility of a SDS micelle (μ_{mc}) which may be determined using Sudan III or dodecanophenone, having a very strong partitioning in the SDS micelle, as a marker. However, the electrophoretic mobility of SDS micelle was not determined in this work. In MEKC using 10 mM phosphate as a buffer, the electrophoretic mobility of SDS micelle was reported to be -4.75×10^{-8} m^2 V^{-1} s^{-1} [Nelson and Lee 1996]. From Figure 3.9, the observed electrophoretic mobilities of analytes at 20 mM SDS are smaller than those at 0 mM SDS because the greater viscosity of the solution and the smaller ionic strength at 20 mM SDS affect a decrease in the electrophoretic mobility. At above 20 mM SDS, the observed electrophoretic mobilities of GA_3 and unknowns 2 and 4 are seen to increase with an increase in the SDS concentration due to an increase in the number of the SDS micelle, leading to the greater mole fraction of the analytes in the micellar phase and the higher electrophoretic mobility ($\mu_{mc} > \mu_A$). A different change of electrophoretic mobility of each analyte is due to the difference in the retention factor of each analyte. Theoretically, the retention factor of analyte linearly increases with an increase in the SDS concentration [Khaledi 1998].

The total mobilities of the analytes in Figure 3.10 are seen to decrease with an increase in the SDS concentration due to insignificantly different EOF and the increase in the electrophoretic mobility. It should be noted that, for negatively charged analytes under high EOF, the greater the electrophoretic mobility, the smaller the total mobility as seen in Figure 1.5.

Table 3.4 shows the effect of the SDS concentration on peak efficiency of GA_3 and resolution for GA_3:unknown 2 and GA_3:unknown 4. Since contribution to peak variance in MEKC is complicated, a comparison between the observed and predicted peak variance is not discussed. At 0 to 40 mM SDS, the peak efficiency (N) of GA_3 could not determined due to the overlapping of GA_3 and unknown 4. An increase in SDS concentration from 50 to 150 mM resulted in an increase in the value of N or a decrease in peak variance ($N \propto 1/\sigma^2$). Theoretically, an increase in SDS concentration can affect the following contributions to the peak variance: (i) an increase in peak variance due to diffusion as an increase of diffusion coefficient and the migration time of GA_3 (see Figures 3.7-3.10 and Equations 1.20-1.22), (ii) an increase in peak variance due to Joule heating as an increase in the ionic strength of the BGE containing higher SDS concentration, (iii) a decrease in peak variance due to EMD as an increase in the ionic strength, and (iv) a decrease in peak variance due to polydispersity, a difference in the number of SDS monomers in a micelle, as a higher SDS concentration [Cole *et al.* 1990]. From Table 3.4, in comparison with CZE without SDS, MEKC with SDS above 50 mM was found to give the smaller peak variance (higher N) of GA_3. Previously work reported that the BGE with higher viscosity than the sample plug resulted in a decrease in a parabolic profile caused by the mismatch of the EOF in the sample plug and BGE, implying a decrease in peak broadening of analytes [Monton *et al.* 2001]. In this work, it is thought that the higher viscosity of the solution resulting from SDS may result in smaller peak variance of analytes in MEKC than CZE. This work showed that an increase of peak variance due to diffusion and Joule heating gave smaller effect than a decrease of peak variance due to EMD, polydispersity and mismatch of EOF. In some cases, an increase in SDS concentration resulted in the fluctuation of N or an increase of N to maximum and then a decrease with higher SDS concentration [Dang *et al.* 1993 and Ahuja *et al.* 1994].

The values of the resolution in Table 3.4 were found to increase with an increase in the SDS concentration due to the greater separation factor (α) as seen in Figure 3.9 which shows the greater difference in the observed electrophoretic mobility. From Equation 1.18, the resolution mainly depends on α-1, therefore, the greater the value of α, the higher the resolution.

It can be concluded that MEKC, and not CZE, can be used for determination of GA_3 in fermentation broth. In MEKC, the resolution of GA_3 may be improved by variation of the BGE pH and the separation temperature and addition of organic solvent. However, MEKC separation in this work was preferred to use a $Na_2B_4O_7$ solution which is a buffer without the use of any reagent for adjusting pH, to separate at temperature of 25° C near the room temperature and to avoid the use of organic solvent. In this study, a decrease in the applied voltage for separation resulted in longer analysis time, and better resolution was not obtained. Therefore, the following MEKC conditions were chosen for determination of GA_3 in the fermentation broth; 25 mM $Na_2B_4O_7$, 100 mM SDS and separation voltage of 30 kV. The baseline resolution of the GA_3 peak and unknown peak 4 was obtained to be 2.13, which is enough for quantitative analysis.

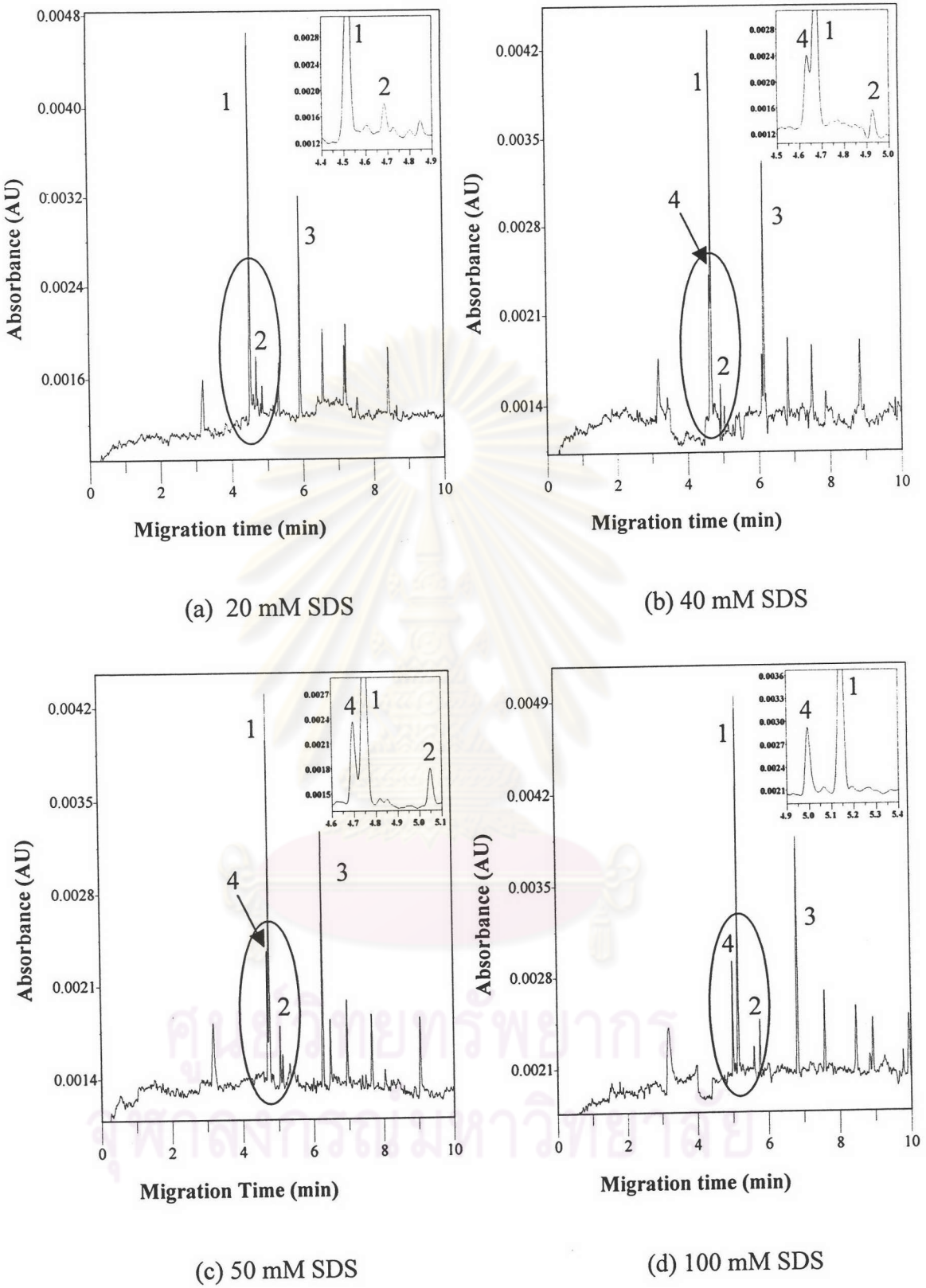

Figure 3.7 An example of electropherograms of 10-day fermentation broth diluted 10 times using (a) 20, (b) 40, (c) 50 and (d) 100 mM SDS, 25 mM $Na_2B_4O_7$ and separation voltage of +30 kV. Peak 1 = GA_3, 2 = unknown, 3 = AMBA and 4 = unknown. Other CE conditions as shown in Figure 3.1.

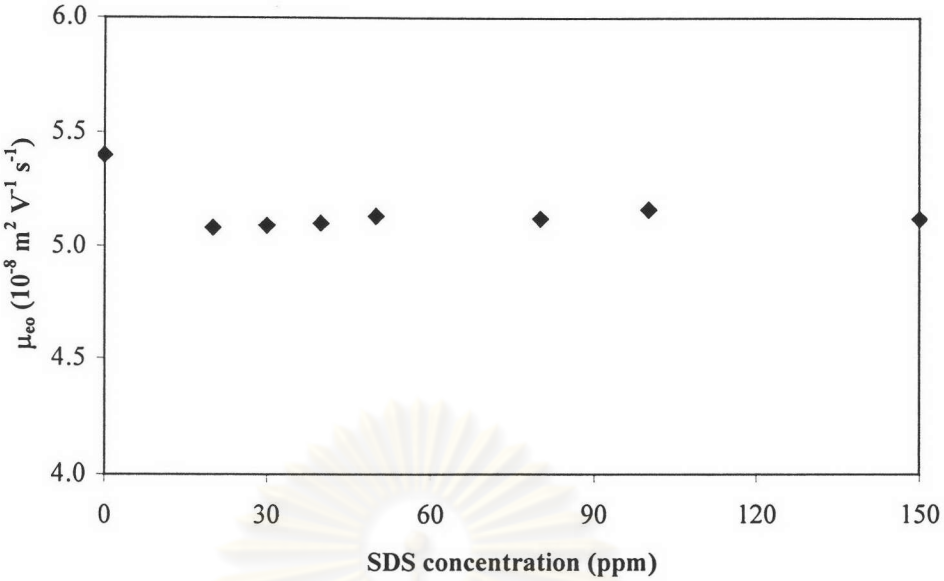

Figure 3.8 Effect of SDS concentration on electroosmotic mobility at separation voltage of +30 kV. Other CE conditions as shown in Figure 3.1.

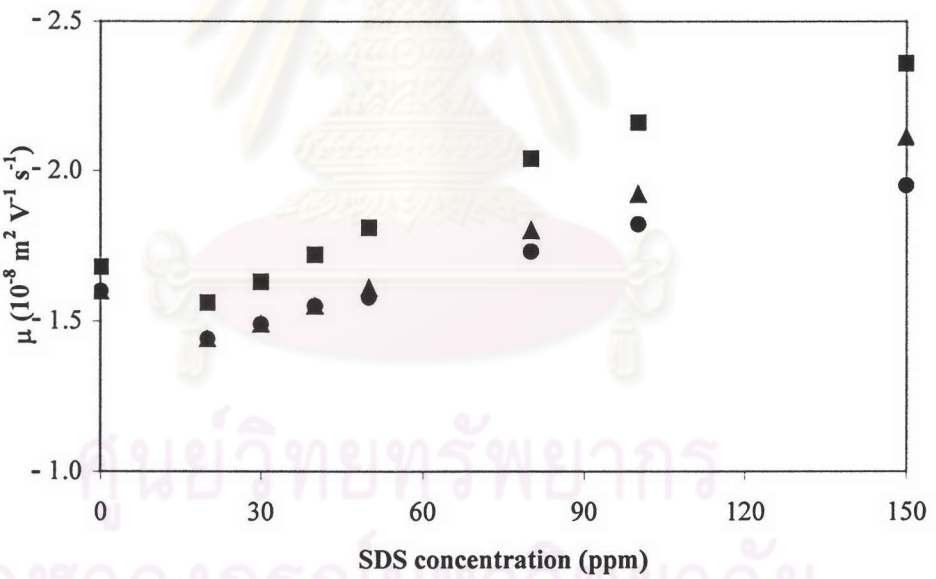

Figure 3.9 Effect of SDS concentration on electrophoretic mobility (μ) of GA_3 (▲), unknown 2 (■) and unknown 4 (●) at separation voltage of +30 kV. Other CE conditions as shown in Figure 3.1.

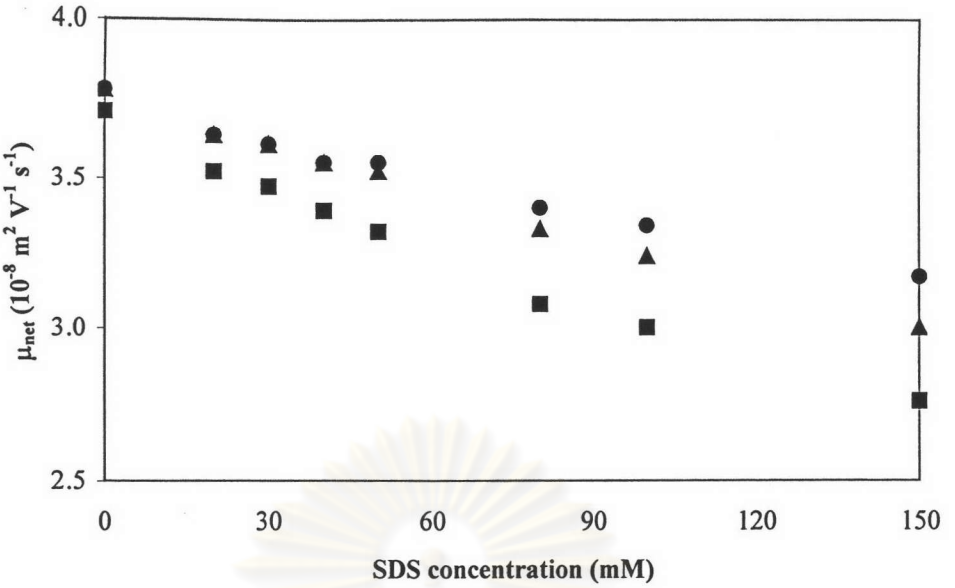

Figure 3.10 Effect of SDS concentration on total mobility (μ_{net}) of GA_3 (▲), unknown 2 (■) and unknown 4 (●) at separation voltage of +30 kV. Other CE conditions as shown in Figure 3.1.

Table 3.4 Effect of SDS concentration on peak efficiency (N) of GA_3 and resolution (R_s) for GA_3:unknown 2 and GA_3:unknown 4

SDS (mM)	R_s		N (10^5)
	GA_3:unknown 2	GA_3:unknown 4	
0	0.93 ± 0.01	0	1.07
20	1.21 ± 0.02	0	*a*
30	1.91 ± 0.10	0	*a*
40	2.27 ± 0.12	<0.5	*a*
50	3.67 ± 0.10	0.59 ± 0.20	*a*
80	4.10 ± 0.10	1.26 ± 0.12	1.66
100	5.07 ± 0.07	2.12 ± 0.04	1.67
150	6.96 ± 0.01	2.95 ± 0.20	2.04

a means overlapped peak

3.1.4 Stability of GA_3 in water and diluted BGE

Typically, the analyte dissolved in the 10 times diluted BGE is used to give sample stacking and the minimum peak variance due to injection length and mismatch of EOF between a sample plug and BGE zone [Burgi and Chien 1991]. However, previous work reported that GA_3 could be decomposed in a basic solution, studied by HPTLC [Kumar and Lonsane 1986]. Therefore, the stability of GA_3 in water and 2.5 mM $Na_2B_4O_7$ was studied at period of time 0 to 48 hours using suitable MEKC conditions obtained from Section 3.1.3. Figure 3.11 shows an example of the electropherograms in GA_3 dissolved in water and 2.5 mM $Na_2B_4O_7$. As previously mentioned, the amount of analyte injected in CE is proportional to A_{corr}. In order to correct imprecision in the amount of analyte injected [Mayer 2001], each GA_3 solution contains 10 ppm AMBA as an internal standard. The A_{corr} ratio of GA_3 and AMBA, $A_{corr,ratio}$, was determined from the MEKC electropherogram. The GA_3 concentration at a given period of time, $C(GA_3)$, is obtained using the equation,

$$C(GA_3) = \frac{100A_{corr,ratio}}{A^0_{corr,ratio}} \qquad (3.8)$$

where $A^0_{corr,ratio}$ is the value of $A_{corr,ratio}$ at the beginning concentration of GA_3 (100 ppm)

Figure 3.12 shows the concentrations of GA_3 in water and a 2.5 mM $Na_2B_4O_7$ solution as a function of the period of time. Each point is the average for triplicate runs. Results in Figure 3.12 suggested that GA_3 in the 2.5 mM $Na_2B_4O_7$ solution was decomposed faster than that in water, especially after the period of time 12 hours. At the period of time 12, 24 and 48 hours, the amounts of GA_3 was found to decrease 14.6, 35.4 and 45.8% for the solution containing 2.5 mM $Na_2B_4O_7$, while 6.3, 11.9 and 17.5% for the solution in pure water. This suggests that the GA_3 standard solutions should be prepared in water, and used for analysis within 12 hours.

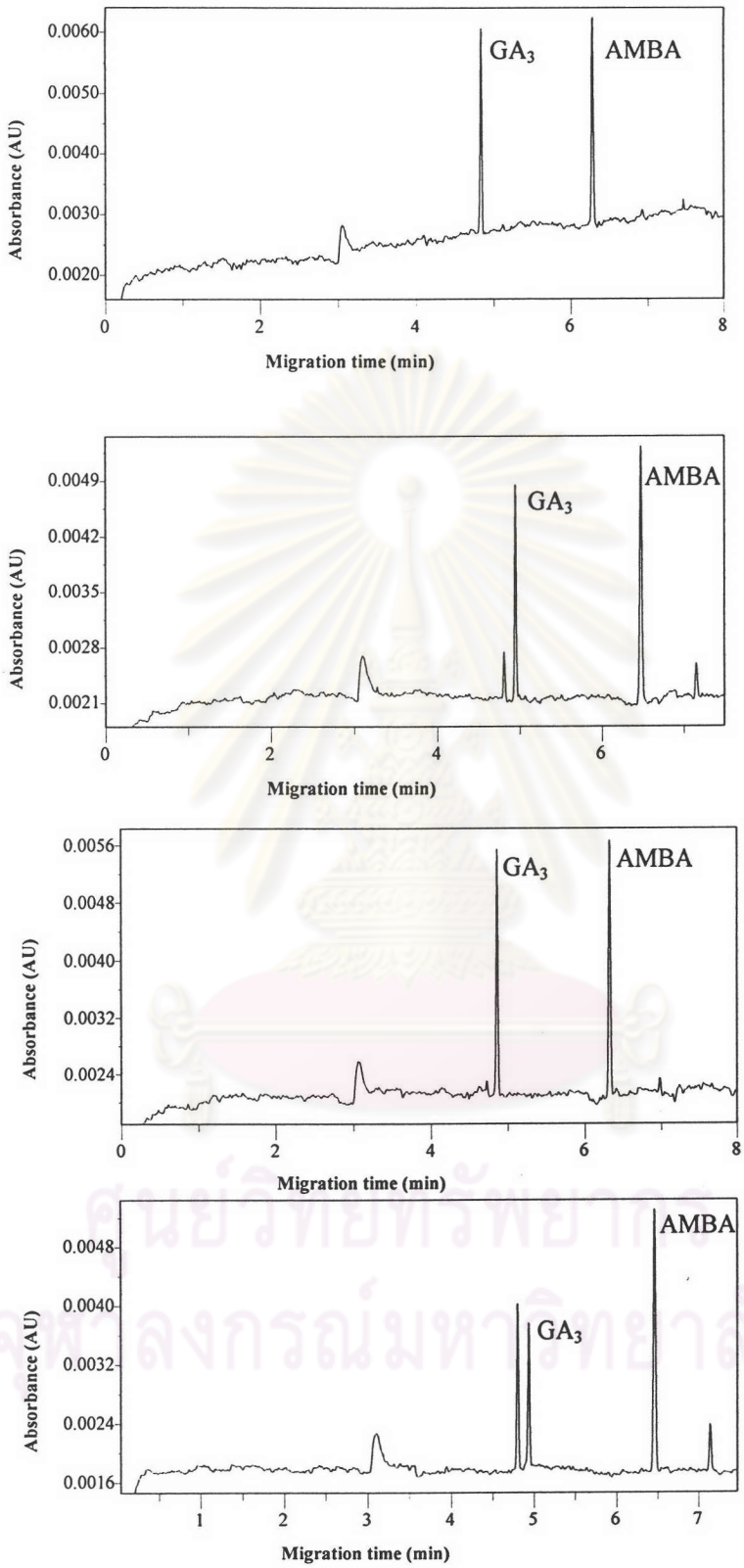

Figure 3.11 An example of electropherograms of GA_3 dissolved in water at the period of time 0 hour (a) and 48 hours (b) and in 2.5 mM $Na_2B_4O_7$ at the period of time 0 hour (c) and 48 hours (d). CE conditions: uncoated fused silica capillary 50 μm I.D. × 57 cm (50 cm to detector), 25 mM $Na_2B_4O_7$, 100 mM SDS, separation voltage of +30 kV, temperature of 25 °C, 0.5 psi pressure injection for 4 s and UV detection at 214 nm.

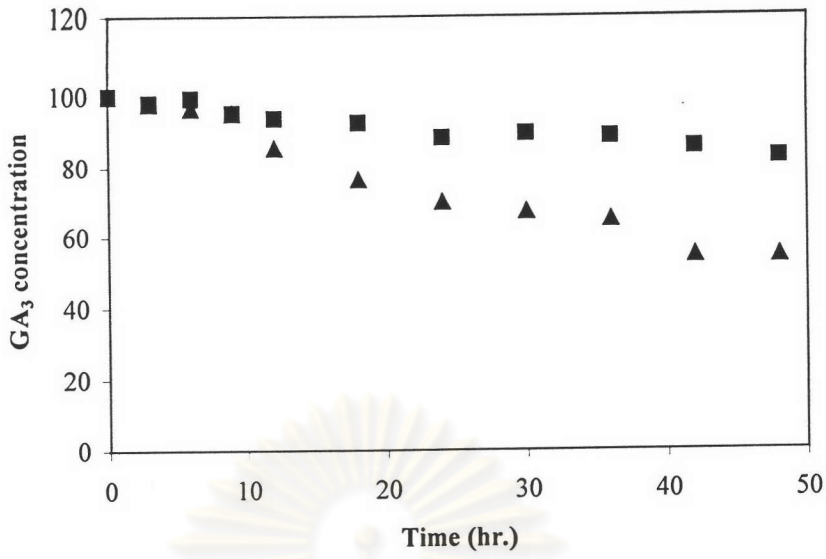

Figure 3.12 The amounts of GA_3 in water (■) and a 2.5 mM $Na_2B_4O_7$ solution (▲) as a function of the period of time.

3.2 Validation of MEKC Method

3.2.1 Calibration plot

In initial study, the concentration range of 20 to 2000 ppm GA_3 in water was used for a calibration plot because the content of GA_3 in the 3 to 10-day fermentation broth was found to be less than 2000 ppm. Each solution also contained 10 ppm AMBA as the internal standard. The relationship between $A_{corr,ratio}$ and the GA_3 concentration was fitted to be linear, giving the equation $y = 0.0085x + 0.0058$, with a high correlation coefficient of $r^2 = 0.9997$, where y is the value of $A_{corr,ratio}$, and x the value of the GA_3 concentration. However, without dilution of the broth, the baseline resolution of GA_3 and unknown peak 4 was not achieved. Therefore, the 10 times diluted broth was prepared for MEKC analysis, and the concentration range of 20 to 200 ppm GA_3 in water was used for a calibration plot using 10 ppm AMBA as the internal standard. An example of an electropherogram of 100 ppm GA_3 containing 10 ppm AMBA is shown in Figure 3.11a. Figure 3.13 shows a plot of the A_{corr} ratio of GA_3 and AMBA as a function of GA_3 concentration. The value of $A_{corr,ratio}$ shown in Figure 3.13 is the average for three runs, with RSD < 3.0 %. The liner relationship in Figure 3.13 gives the equation $y = 0.010x + 0.0323$, with a high value of $r^2 = 0.9990$.

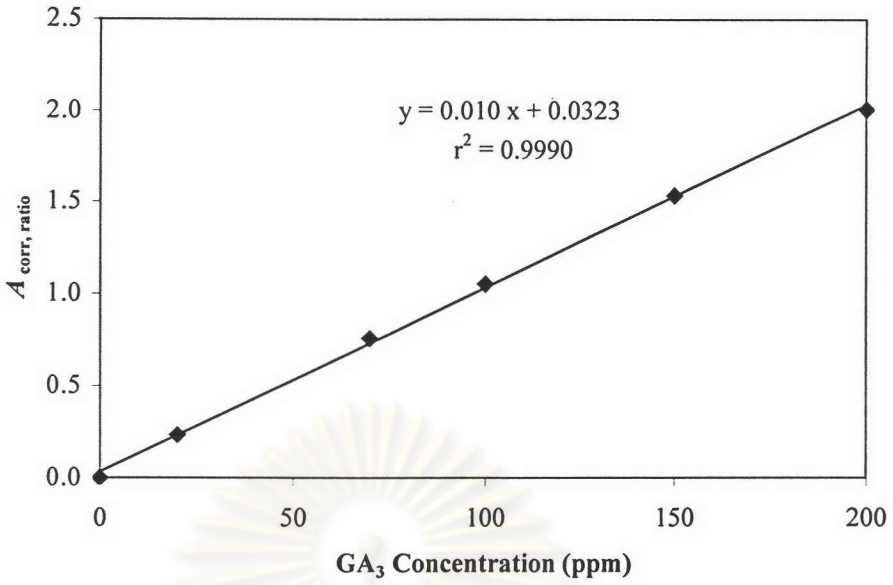

Figure 3.13 A plot of the A_{corr} ratio of GA_3 and AMBA ($A_{corr,ratio}$) a function of GA_3 concentration.

3.2.2 Accuracy and precision

The known amounts of GA_3 spiked in water and 10 times diluted fermentation broth were used to study accuracy and precision of the method and to investigate the effect of sample matrix on accuracy and precision. Each experiment was caried out by MEKC for 10 replicates. For GA_3 spiked in water, the known amounts of GA_3 at levels of 50 and 140 ppm were used. The determined amount of GA_3 was obtained from the measured $A_{corr,ratio}$ and the calibration established in Figure 3.13. For GA_3 spiked in the diluted broth, the amount of GA_3 at a level of 50 ppm in 5, 7, and 10-day fermentation broths was used. At the level of 140 ppm of GA_3 spiked in the diluted broth resulted in a larger peak of GA_3 and overlapping peaks of GA_3 and unknown peak 4, leading to inaccuracy in integrated peak area. The determined amount of GA_3 spiked in the diluted broth is equal to the total determined amounts of GA_3, after spiking GA_3, subtracting the average determined amount of GA_3 in the diluted broth without spiking GA_3. Results of the amounts of GA_3 spiked in the water and diluted broths are shown in Table 3.5. The values of recovery were found in the range of 95 to 100% with RSD < 5%, indicating high accuracy and precision of the MEKC method, respectively. In addition, the sample matrix was found to give no effect on the accuracy and precision of the method due to insignificantly different values of recovery and RSD for GA_3 spiked in water and the diluted broth.

Tables 3.6 and 3.7 show results of the migration time (t_{GA3}), electrophoretic mobility (μ_{GA3}) and corrected peak area (corr. A_{GA3}) of GA_3 within a day and 5 days, using 140 ppm GA_3 standard solution. Each value in Table 3.6 was obtained from each run within a day for 10 runs. Each value for day-to-day in Table 3.7 was obtained from the average for triplicate runs. Both within a day and day-to-day, the values of RSD of t_{GA3} and μ_{GA3} were found to be less than 1 %, indicating that high precision in the migration time and the electrophoretic mobility of GA_3 in MEKC. This is a benefit from the use of $Na_2B_4O_7$ as the BGE which provides high capacity buffer and constant pH leading to stable EOF and electrophoretic mobility of analyte, as previously mentioned in Section 3.1.1. From Tables 3.6 and 3.7, the values of corr. A_{GA3} within a day and 5 days were insignificantly different, with RSD < 5 %. These indicate that high precision in corrected peak area of GA_3 in MEKC is obtained.

Table 3.5 The determined and actual amounts of GA_3 spiked in water and the fermentation broths diluted 10 times

Matrix	The amount of GA_3 (ppm)		Recovery (%)	RSD (%)
	Spiked	Determined		
Water	50.0	47.6 ± 1.9	95.1 ± 4.0	4.0
	140.0	136.0 ± 2.2	97.1 ± 1.5	1.6
Diluted 5-day broth	50.0	48.8 ± 2.2	97.6 ± 4.4	4.5
Diluted 7-day broth	50.0	50.0 ± 1.7	100.0 ± 3.4	3.4
Diluted 10-day broth	50.0	47.6 ± 2.0	95.2 ± 4.1	4.3

Table 3.6 Within-day migration time, electrophoretic mobility and corrected peak area of GA_3. MEKC conditions as shown in Figure 3.11.

No.	t_{GA3} (min)	μ_{GA3} (10^{-8} m^2 V^{-1} s^{-1})	corr. A_{GA3} (μAU)
1	4.880	-1.918	23.93
2	4.878	-1.915	23.58
3	4.878	-1.933	24.70
4	4.877	-1.908	24.63
5	4.878	-1.912	24.64
6	4.878	-1.907	23.96
7	4.880	-1.901	24.40
8	4.880	-1.916	24.30
9	4.882	-1.918	24.61
10	4.883	-1.915	24.28
average	4.879 ± 0.002	-1.914 ± 0.009	24.31 ± 0.37
%RSD	0.04	0.45	1.54

Table 3.7 Day-to-day migration time, electrophoretic mobility and corrected peak area of GA_3 (n = 5 days). MEKC conditions as shown in Figure 3.11.

Day	t_{GA3} (min)	μ_{GA3} (10^{-8} m^2 V^{-1} s^{-1})	corr. A_{GA3} (μAU)
1	4.865 ± 0.004	-1.901 ± 0.008	24.43 ± 0.48
2	4.879 ± 0.001	-1.922 ± 0.010	24.07 ± 0.57
3	4.831 ± 0.010	-1.912 ± 0.004	25.41 ± 0.22
4	4.790 ± 0.003	-1.909 ± 0.006	26.61 ± 0.15
5	4.910 ± 0.003	-1.926 ± 0.004	25.57 ± 0.07
average	4.855 ± 0.031	-1.914 ± 0.010	25.22 ± 0.98
%RSD	0.65	0.56	3.88

Each value is obtained from the average for triplicate runs.

3.2.3 Limit of detection (LOD) and limit of quantitation (LOQ)

LOD and LOQ were defined as the analyte concentration at signal-to-noise ratios of 3 and 10, respectively. For GA_3 determined using this method, LOD and LOQ were found to be 5.0 and 10.0 ppm, respecively. LOD may be improved by using a bubble cell capillary to increase cell path length or large volume sample stacking as an on-column pre-concentration [Liu *et al.* 2002]. However, it is not necessary for this work where the amount of GA_3 in the fermentation broth is greater than 20 ppm.

3.3 HPLC Analysis

3.3.1 Recovery of GA_3 extraction

As previously mentioned, HPLC analysis of GA_3 in the fermentation broth requires sample preparation using liquid extraction with ethylacetate as the procedure reported by Samappito [1994]. However, the recovery of GA_3 extraction has not been previously reported. In this work, the recovery of GA_3 extraction with ethylacetate was determined as the procedure in the Section 2.4.4. Figure 3.14 shows an example of a chromatogram of 600 ppm GA_3 standard solution containing 100 ppm AP. Figure 3.15 shows an example of HPLC chromatograms of GA_3 extracted from the 10-day fermentation broth with and without spiking the known amount of GA_3 standard. AP was used as a surrogate to compare the recovery of GA_3 and AP. Figures 3.16 shows calibration plots between peak area of GA_3 (3.16a) and the ratio of peak area of GA_3 to that of AP (3.16b) as a function of GA_3 concentration in the range of 200 to 1200 ppm. The amount of GA_3 extracted from the fermentation broth was obtained by measuring peak area of GA_3 and using an equation, $y = 21191x + 3965$ with $r^2 = 0.9999$, obtained from a calibration plot in Figure 3.16. The recovery of spiked GA_3 was calculated by the similar way used in CE as mentioned in Section 3.2.2. Table 3.8 shows a comparison of the spiked and determined amount of GA_3 in the 5 and 10-day fermentation broths. The determined amount of GA_3 spiked in the broths, directly obtained from peak area of GA_3, gave values of the GA_3 recovery of 62.5 ± 8.1 and 56.5 ± 3.8 %, with RSD 13.0 and 6.7 %, for the 5 and 10-day fermentation broths,

respectively. This indicates that ~40 % GA_3 lose during the extraction, and poor precision in the values of the GA_3 recovery is obtained with RSD > 5 %.

The recovery of AP used as a surrogate was calculated from 100 multiplied by the ratio of peak area of AP spiked in the broth to that in the GA_3 standard solution. The recovery of AP extraction was found to be 65.2 ± 2.7 and 64.3 ± 1.6 % for the 5 and 10-day fermentation broths, respectively. The similar range for the extraction recovery of GA_3 and AP imply that the amount of GA_3 in the broth may be corrected using the extraction recovery of AP. The corrected amounts of GA_3 in the fermentation broths determined by HPLC were found to be 264.4 ± 19.4 and 234.2 ± 16.4 ppm, for the 5 and 10-day fermentation broths, respectively, which are close to the spiked amount of 250 ppm. Therefore, for analysis of GA_3 in the broths by HPLC, the amount of GA_3 should be corrected using the extraction recovery of AP determined in each batch.

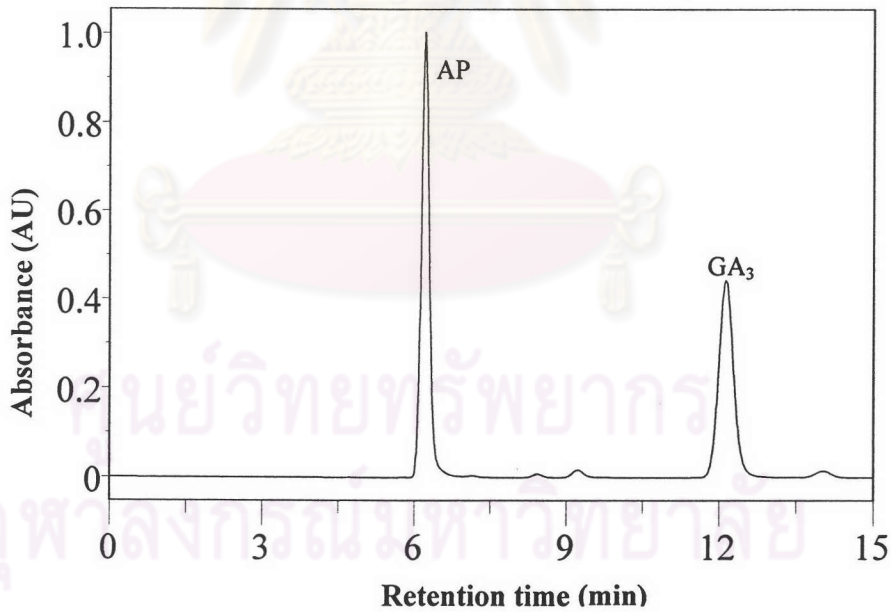

Figure 3.14 An example of a chromatogram of 600 ppm GA_3 standard solution containing 100 ppm AP.

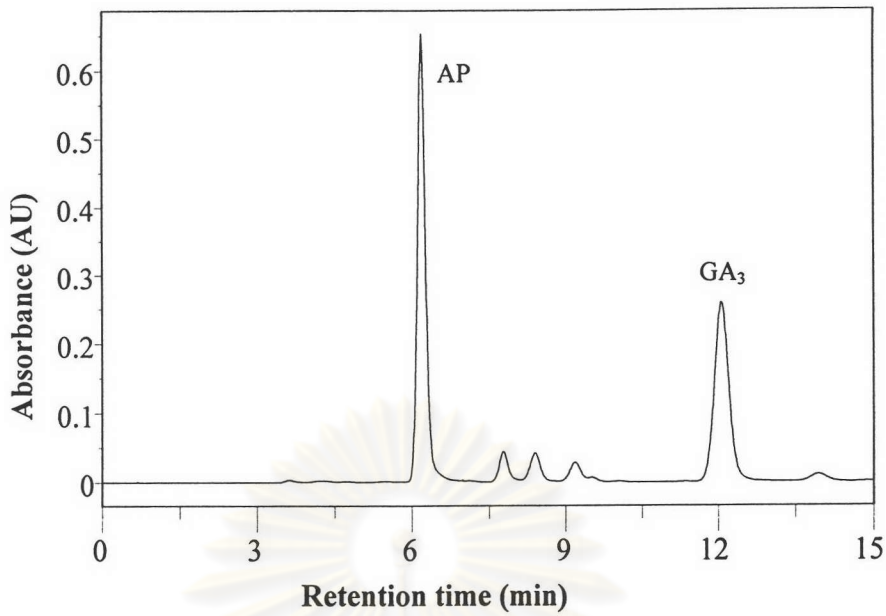

(a) without spiking 250 ppm

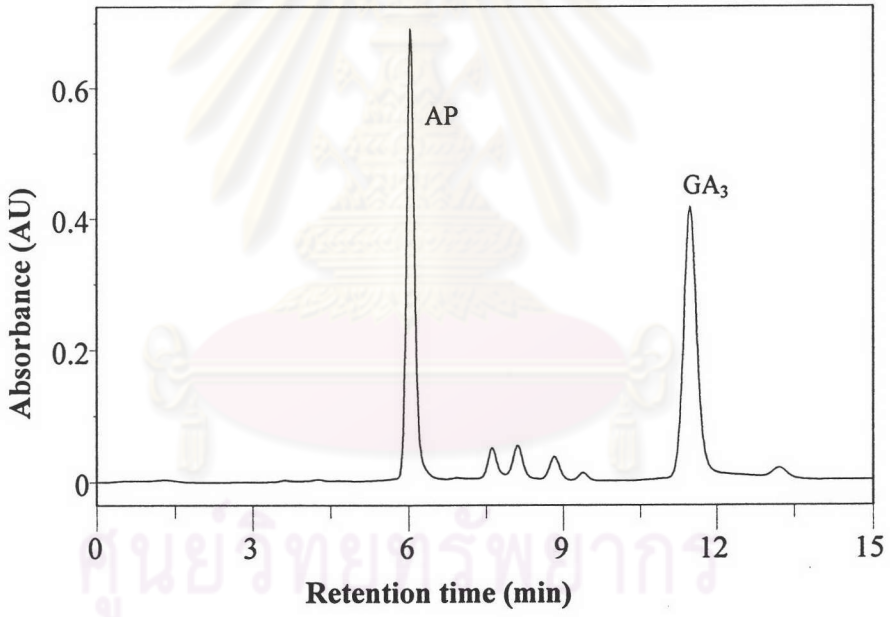

(b) with spiking 250 ppm

Figure 3.15 An example of HPLC chromatograms of GA_3 extracted from the 10-day fermentation broth without (a) and with (b) spiking 250 ppm GA_3 standard.

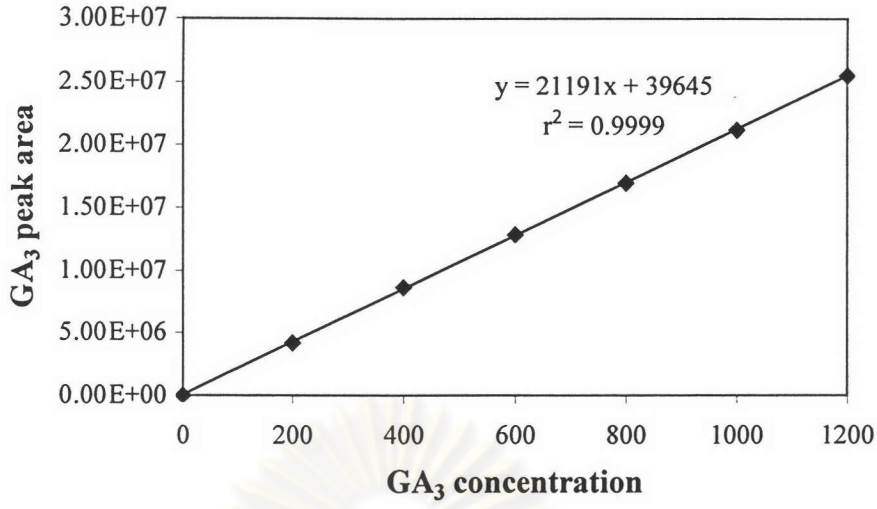

Figure 3.16 Calibration plots between peak area of GA_3 as a function of GA_3 concentration in the range of 200 to 1200 ppm.

Table 3.8 The determined and actual amounts of GA_3 spiked in 5 and 10-day fermentation broths obtaining from HPLC

Broth	The amount (ppm)				Extraction recovery (%)	
	Spiked		Determined[a]			
	GA_3	AP	GA_3	AP	GA_3	AP
5 days	250	100	156.3 ± 20.3	65.2 ± 2.7	62.5 ± 8.1	65.2 ± 2.7
10 days	250	100	141.3 ± 9.4	64.3 ± 1.6	56.5 ± 3.8	64.3 ± 1.6

[a] the average of triplicate batchs and triplicate HPLC runs

3.3.2 Limit of detection (LOD) and limit of quantitation (LOQ)

For HPLC analysis, LOD and LOQ for GA_3 were found to be 0.5 and 2.0 ppm, respectively. It can be seen that LOD for GA_3 obtained from HPLC is better than that from CE (5.0 ppm). In this work, the path length of the detection cell in HPLC is 1 cm, while ~50 μm in CE. Therefore, the larger the path length, the better the detection sensitivity.

3.4 Applications to Real Samples

3.4.1 Determination of GA_3 in fermentation broth by MEKC and HPLC

The amounts of GA_3 in the 3, 5, 7,10 and 11-day fermentation broths determined by MEKC and HPLC were compared. For MEKC analysis using conditions shown in Section 3.1.3, the broths were filterred and ten times diluted with water. The concentration of GA_3 in the diluted broth was obtained from the ratio of the corrected peak areas of GA_3 and AMBA and the calibration plot in Figure 3.13. For HPLC analysis, sample preparation was carried out using the procedure as described in Section 2.2.2. Figures 3.17 and 3.18 show an example of HPLC chromatograms and MEKC electropherograms of 5 and 10-day fermentation broths, respectively. Table 3.9 shows a comparison of GA_3 in the broth determined by MEKC and HPLC. For HPLC analysis, the determined amount of GA_3 was obtained from the peak area of GA_3 and the calibration plot in Figure 3.16. The corrected amount of GA_3 was obtained from 100 × the determined amount/the recovery of AP. From Table 3.9, the determined amount of GA_3 from HPLC analysis is seen to be less than the amount of GA_3 determined by MEKC, due to the loss of GA_3 during the extraction prior to HPLC injection as previously mentioned. From Table 3.9, for each broth, the amount of GA_3 determined by MEKC is seemed to be in agreement with the corrected amount of GA_3 determined by HPLC. Figure 3.19 shows relationship of the amounts of GA_3 in 3 to 11-day fermentation broths obtained from MEKC and HPLC (corrected amount using the extraction recovery of AP). In addition, a slope value of 0.987 in Figure 3.19, very close to 1.0, indicates that good agreement is obtained between the amounts of GA_3 determined by MEKC and HPLC. Therefore, MEKC can be used as an alternative technique to HPLC for analysis of GA_3 in the fermentation broth.

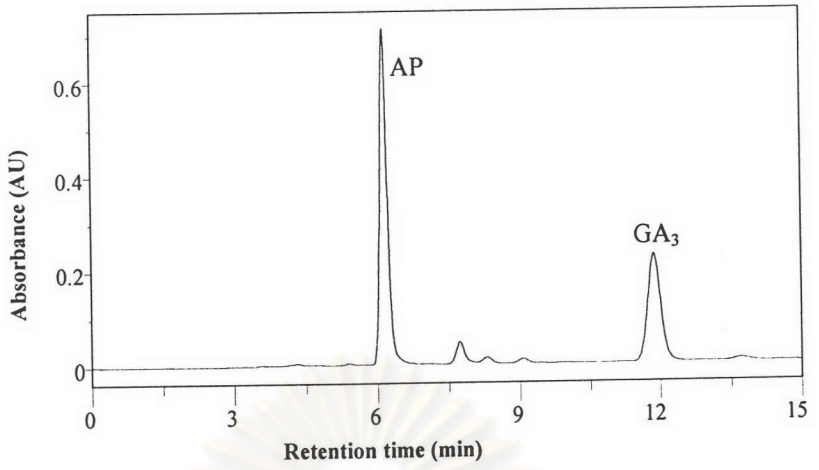

(a) 5-day fermentation broth

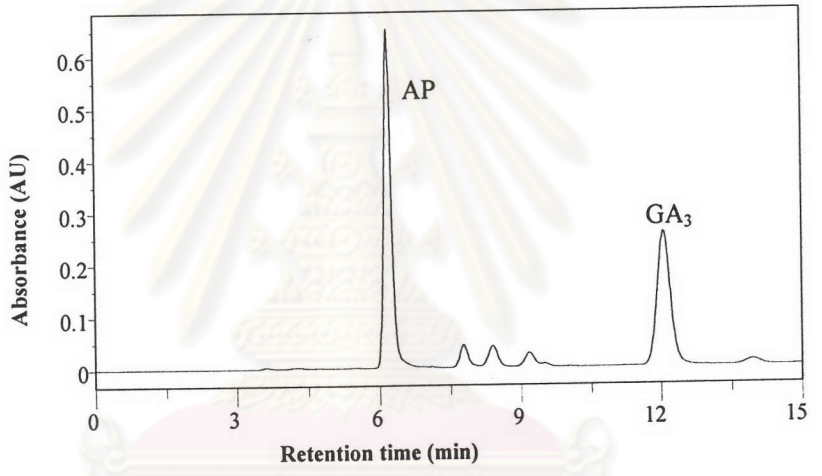

(b) 10-day fermentation broth

Figure 3.17 An example of HPLC chromatograms of the 5 (a) and 10-day (b) fermentation broths.

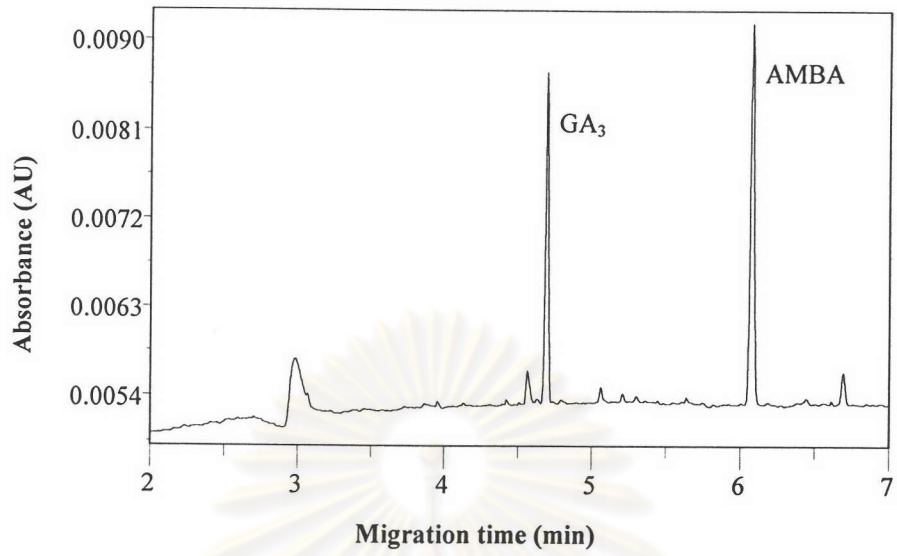

(a) 5-day fermentation broth

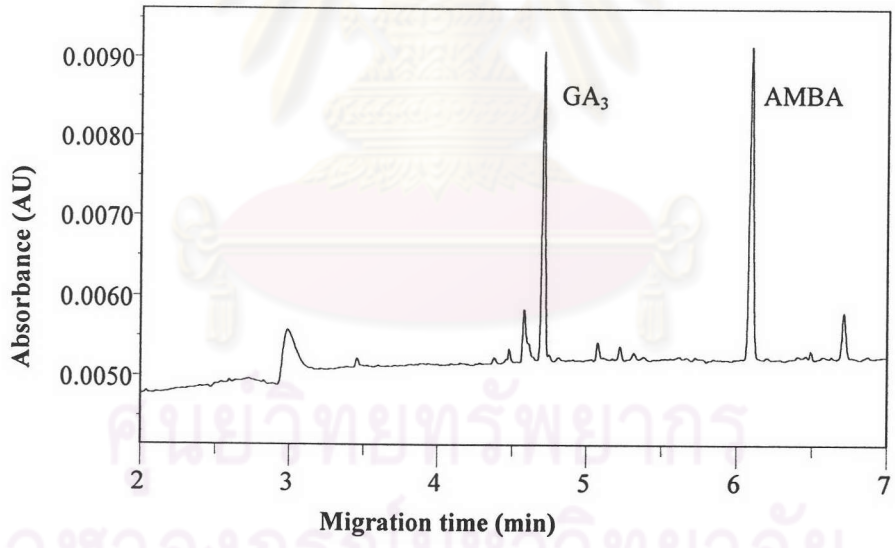

(b) 10-day fermentation broth

Figure 3.18 An example of MEKC electropherograms of the 5 (a) and 10-day (b) fermentation broths. CE conditions as shown in Figure 3.11.

Table 3.9 A comparison of GA_3 in the broths determined by MEKC and HPLC

Broth	The amount of GA_3 (ppm) determined by		
	MEKC	HPLC	
		Determined	Corrected[a]
3 days	384.1 ± 18.4	275.5 ± 5.4	393.0 ± 5.4
5 days	696.9 ± 11.0	487.7 ± 11.9	724.2 ± 7.3
7 days	780.6 ± 12.9	517.9 ± 22.4	773.0 ± 25.0
10 days	878.7 ± 4.1	537.5 ± 22.3	854.0 ± 12.8
11 days	883.5 ± 19.1	624.1 ± 2.7	882.9 ± 1.7

Each value is the average of triplicate bacths of the broth and triplicate runs.
[a]the corrected amount using the AP recovery for each batch extraction

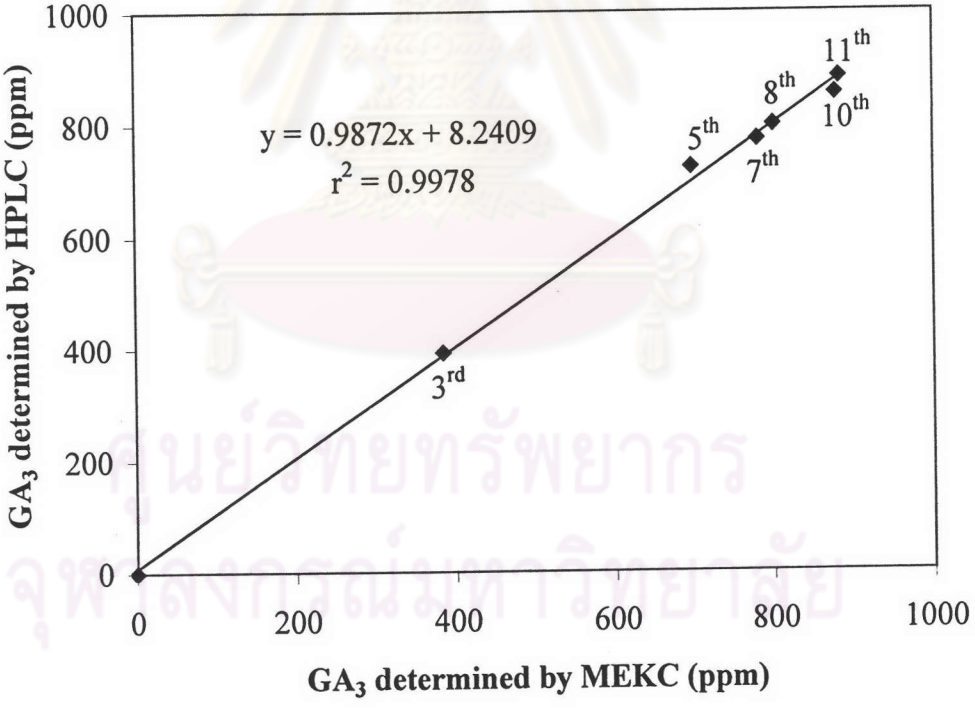

Figure 3.19 Relationship of the amounts of GA_3 in the 3 to 11-day fermentation broths determined by MEKC and HPLC.

3.4.2 Determination of GA_3 in a commercial products by CZE and MEKC

For GA_3 products, there are two types of CU Gibb. packages, a tablet of GA_3 and a tube of GA_3. The actual weight of a GA_3 tablet and a GA_3 tube were determined (~1.0 g and ~1.43 g, respectively). The GA_3 tablet was grinded before preparation. The solutions of GA_3 tablet and GA_3 tube were prepared by weighing the appropriate amount of GA_3 tablet (~0.0100 g) and GA_3 tube (~0.0286 g) and then dissolving this in 10 ml water. Each sample solution contained 10 ppm AMBA as an internal standard. The amounts of GA_3 were determined by CZE and MEKC. For CZE analysis, CZE conditions obtained from Section 3.1.2 were used to determine GA_3 in commercial products. Figures 3.20 and 3.21 show an example of electropherograms of the GA_3 tablet and GA_3 tube determined by CZE and MEKC, respectively. The amount of GA_3 in a solution (C) is obtained from the ratio of the measurement of corrected peak areas of GA_3 and AMBA and an equation, $y = 0.0130+0.0031$ with $r^2 = 0.9999$, from a calibration plot of the ratio of the corrected peak areas of GA_3 and AMBA as a function of the concentration of GA_3. For MEKC analysis, the amount of GA_3 in a solution is obtained from the ratio of the measurement of corrected peak areas of GA_3 and AMBA and the calibration plot in Figure 3.13. The percentage, P (%w/w), of GA_3 in commercial product is obtained from the equation

$$P\,(\%\text{w/w}) = \frac{fC\,(\text{ppm}) \times V\,(\text{ml})}{10 \times w\,(\text{mg})} \qquad (3.9)$$

where C is the amount of GA_3 in a solution (ppm), V the volume of the GA_3 solution (ml), w the desired weight of GA_3 tablet or tube (mg), and f the dilution factor. The amount of GA_3 in commercial product in unit of mg/tablet or mg/tube is calculated from the equation

$$\text{mg/tablet or mg/tube} = \frac{W\,(\text{mg}) \times P\,(\%\text{w/w})}{100} \qquad (3.10)$$

where W is the total weight of a GA_3 tablet or tube (mg).

Tables 3.10 and 3.11 show a comparision of GA_3 in the CU Gibb tablets and tubes, respectively, determined by CZE and MEKC. From Tables 3.10 and 3.11, the amounts of GA_3 in the tablets and tubes determined by CZE and MEKC were found to be insignificantly different. Using MEKC analysis, a small peak, similar to unknown 4 in the fermentation broth, near GA_3 peak was observed for the CU Gibb tablet, while was not found for the CU Gibb tube. Result from Section 3.1.4 showed that the unknown 4 was obtained from the decomposition of GA_3. The reason of the absence of unknown 4 in the CU Gibb tubes may be because the fresh samples of the CU Gibb tubes were used for analysis. Although the amounts of GA_3 in the CU Gibb determined by MEKC and CZE were found to be insignificantly different, MEKC analysis provides more reliable than does CZE because CZE cannot separate GA_3 and unknown 4.

The labeled amounts of GA_3 are 50 mg/tube and 100 mg/tablet. Using MEKC analysis, the average determined amounts of GA_3 were found to be 56.9 ± 6.8 mg/tube and 107.0 ± 5.8 mg/tablet. It is the fact that the actual amount of GA_3 in CU Gibb products is typically 5 to 10 % higher than the labeled amount in order to compensate decomposition of GA_3 during production and storage. Thus, good agreement is obtained between determined and actual amounts of GA_3 in commercial products.

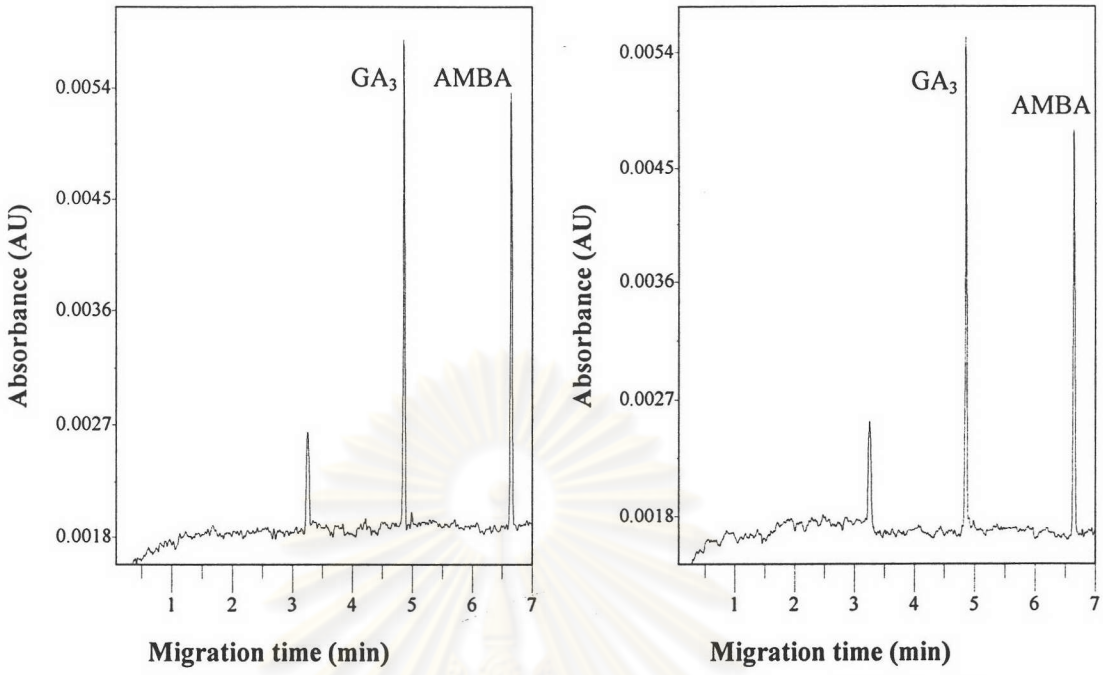

Figure 3.20 An example of CZE electropherograms of the GA_3 tablet (a) and GA_3 tube (b). CE conditions: uncoated fused silica capillary 50 μm I.D. × 57 cm (50 cm to detector), 40 mM $Na_2B_4O_7$, separation voltage of +30 kV, temperature of 25 °C, 0.5 psi pressure injection for 4 s and UV detection at 214 nm.

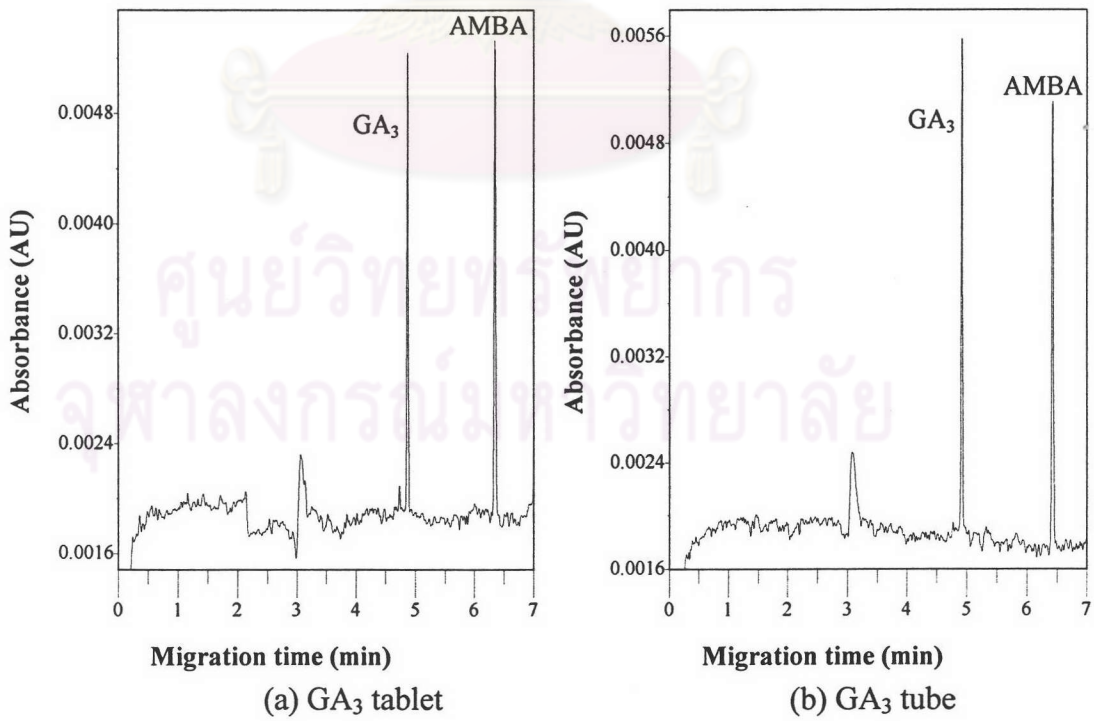

Figure 3.21 An example of MEKC electropherograms of the GA_3 tablet (a) and GA_3 tube (b). CE conditions as shown in Figure 3.11.

Table 3.10 A comparison of GA_3 in the tablet of GA_3 determined by CZE and MEKC

CU Gibb	GA_3 (%w/w)		GA_3 (mg/tablet)		RSD (%)	
	CZE	MEKC	CZE	MEKC	CZE	MEKC
Tablet 1	10.16 ± 0.24	**9.91 ± 0.03**	100.0 ± 2.4	**98.6 ± 0.3**	2.4	**0.3**
Tablet 2	11.02 ± 0.00	**10.99 ± 0.04**	109.6 ± 0.0	**109.5 ± 0.4**	0.0	**0.4**
Tablet 3	11.21 ± 0.17	**10.91 ± 0.05**	110.9 ± 0.8	**108.4 ± 0.5**	0.7	**0.5**
Tablet 4	11.61 ± 0.07	**11.17 ± 0.26**	115.9 ± 0.7	**111.6 ± 2.6**	0.6	**2.3**
Average	11.00 ± 0.58	**10.75 ± 0.53**	109.4 ± 5.8	**107.0 ± 5.4**	5.3	**5.0**

Table 3.11 A comparison of GA_3 in the tube of GA_3 determined by CZE and MEKC

CU Gibb	GA_3 (%w/w)		GA_3 (mg/tube)		RSD (%)	
	CZE	MEKC	CZE	MEKC	CZE	MEKC
Tube 1	4.12 ± 0.13	**3.83 ± 0.04**	58.3 ± 0.6	**54.8 ± 0.6**	1.0	**1.1**
Tube 2	4.09 ± 0.06	**4.06 ± 0.04**	58.5 ± 0.9	**58.0 ± 0.6**	1.5	**1.1**
Tube 3	4.11 ± 0.03	**4.04 ± 0.09**	58.8 ± 0.5	**57.8 ± 1.3**	0.9	**2.2**
Average	4.11 ± 0.08	**3.98 ± 0.13**	58.5 ± 0.6	**56.9 ± 1.7**	1.2	**3.0**